CHEMISTRY OF MATERIALS
Article

Chem. Mater. **2009,** *21,* 3479–3484 3479
DOI:10.1021/cm900225p

Enhanced Photocatalysis of Electrospun Ag−ZnO Heterostructured Nanofibers

Dandan Lin, Hui Wu, Rui Zhang, and Wei Pan*

State Key Laboratory of New Ceramics and Fine Processing, Department of Materials Science and Engineering, Tsinghua University, Beijing 100084, People's Republic of China

Received July 14, 2008. Revised Manuscript Received June 23, 2009

A unique dimer-type heterostructure of Ag−ZnO nanofibers with a diameter of 80−150 nm and coupled Ag nanoparticles in the size range from several to 15 nm have been fabricated by a facile electrospinning method. Rhodamine B (RhB) was employed as a representative dye pollutant to evaluate the ultraviolet (UV) photocatalytic activity of Ag−ZnO nanofibers. It was found that the heterojunction structure promoted the charge separation as well as the photon efficiency, allowing both the photogenerated electrons and holes to participate in the overall photocatalytic reaction. The optimal photocatalytic activity of Ag−ZnO nanofibers exceeded that of pure ZnO nanofibers by a factor of more than 25. A possible mechanism for the enhanced photocatalytic activity of ZnO by Ag was proposed.

Introduction

During the past decades, environmental problems such as air and water pollution have provided the impetus for sustained fundamental and applied research in the area of environmental remediation.[1] With the steady and fast growing field of nanoscience and nanotechnology, nanostructured zinc oxide (ZnO) has become a promising photocatalyst for its high catalytic activity, low cost, and environmental friendliness.[2−5] Major limitation to achieving high photocatalytic efficiency in the ZnO nanostructure systems is the quick recombination of charge carriers. The design and modification of ZnO photocatalysts with high sensitivity and reactivity has attracted much attention. It was found that the photocatalytic performance can be greatly improved by developing ZnO-based heterostructures or composites.[6−9] For instance, Kim et al.[7] have reported improved photocatalytic activity of a zincoxysulfide (ZnO_xS_{1-x}) composite due to its superior visible-light absorptivity over pure ZnS and ZnO. Similarly, coupled ZnO−SnO_2 nanoparticles were found to enhance photocatalytic activity by about 1.3 times as compared with the pure ZnO and 21.3 times with SnO_2.[8]

The prospect of developing novel photocatalysts of metal silver hybridized with ZnO boosts relevant research because of the increase in the rate of electron-transfer process by silver.[10−16] Methods including microwave radiation,[10] coordination homogeneous coprecipitation,[12] hydrothermal synthesis,[14] and solvothermal method[15] have been used to successfully synthesize the Ag−ZnO nanocrystals. The prepared ultrafine catalysts with sizes of several nanometers always present a superior activity due to the large surface-to-volume ratios. However, in a practical photocatalytic process, the separation of these powder photocatalysts from solution after reaction could be very difficult, and meanwhile, the tendency to agglomerate into larger particles will result in a reduction of the photocatalytic activity during the cycling use. Fibril photocatalysts have taken an advantage over spherical powder catalysts for easier separation from solution

*To whom correspondence should be addressed. Tel.: 86-10-62772858. Fax: 86-10-62771160. E-mail: panw@mail.tsinghua.edu.cn.

(1) (a) Zhao, J. C.; Wu, T. X.; Wu, K. Q.; Oikawa, K.; Hidaka, H.; Serpone, N. *Environ. Sci. Technol.* **1998**, *32*(16), 2394–2400. (b) Ohtani, B. *Chem. Lett.* **2008**, *37*(3), 216–229. (c) Hoffmann, M. R.; Martin, S. T.; Choi, W.; Bahnemann, D. W. *Chem. Rev.* **1995**, *95*, 69–96. (d) Ollis, D. F.; Al-Ekabi, H. *Photocatalytic Purification and Treatment of Water and Air*; Elsevier Science Publishers B.V.: Amsterdam, 1993. (e) Hogfelt, A.; Graetzel, M. *Chem. Rev.* **1995**, *95*, 49–68.
(2) Li, D.; Haneda, H. *Chemosphere* **2003**, *51*(2), 129–137.
(3) Yang, J. L.; An, S. J.; Park, W. I.; Yi, G. C.; Choi, W. *Adv. Mater.* **2004**, *16*(18), 1661–1664.
(4) Chakrabarti, S.; Dutta, B. K. *J. Hazard. Mater.* **2004**, *112*(3), 269–278.
(5) Pal, B.; Sharon, M. *Mater. Chem. Phys.* **2002**, *76*(1), 82–87.
(6) He, Y. J.; Yu, X. Y.; Li, T. L.; Yan, L. Y.; Yang, B. L. *Powder Technol.* **2006**, *166*, 72–76.
(7) Kim, C.; Doha, S. J.; Leea, S. G.; Leea, S. J.; Kima, H. Y. *Appl. Catal., A* **2007**, *330*, 127–133.
(8) Wang, C.; Wang, X. M.; Xu, B. Q.; Zhao, J. C.; Mai, B. X.; Peng, P. A.; Sheng, G. Y.; Fu, J. M. *J. Photochem. Photobiol. A* **2004**, *168*, 47–52.
(9) Zhang, M. L.; An, T. C.; Hu, X. H.; Wang, C.; Sheng, G. Y.; Fu, J. M. *Appl. Catal., A* **2004**, *260*, 215–222.
(10) Bhattacharyya, S.; Gedanken, A. *J. Phys. Chem. C* **2008**, *112*(3), 659–665.
(11) Wang, R. H.; Xin, J. H. Z.; Yang, Y.; Liu, H. F.; Xu, L. M.; Hu, J. H. *Appl. Surf. Sci.* **2004**, *227*, 312–317.
(12) Zhou, G.; Deng, J. C. *Mater. Sci. Semicond. Process.* **2007**, *10*, 90–96.
(13) Gouvêa, C. A. K.; Wypych, F.; Moraes, S. G.; Durân, N.; Peralta-Zamora, P. *Chemosphere* **2000**, *40*, 427–432.
(14) Zhang, Y. Y.; Mu, J. *J. Colloid Interface Sci.* **2007**, *309*, 478–484.
(15) Zheng, Y. H.; Zheng, L. R.; Zhan, Y. Y.; Lin, X. Y.; Zheng, Q.; Wei, K. M. *Inorg. Chem.* **2007**, *46*, 6980–6986.
(16) Height, M. J.; Pratsinis, S. E.; Mekasuwandumrong, O.; Praserthdam, P. *Appl. Catal., B* **2006**, *63*, 305–312.

Published on Web 07/14/2009

by filtration or sedimentation.[17] In recent years, electrospun fibrous materials were found to show unique properties suitable for use as catalysts. The main benefits include flexibility of form, three-dimensional open structure, large specific surface area, easy scale-up, and reusability. Photocatalysts with high efficiency and/or selectivity, such as bicomponent TiO_2/SnO_2 nanofibers,[18,19] porous silica/silver nanofibers,[20] silver/TiO_2 nanofibers,[21] and polyacrylamidoxime nanofibers,[22] have been fabricated by electrospinning, fully demonstrating the feasibility and simplicity of this technique.

Accordingly, in this paper, we developed a facile method that combines electrospinning technique with heat treatment to prepare Ag−ZnO heterostructure nanofibers. The catalytic efficiency was evaluated by degradation of Rhodamine B (RhB) dye under UV irradiation, and the reaction state can be easily detected using a simple UV−vis spectroscopy method. To have an in-depth understanding of the photocatalytic mechanism of this heterostructure, the relationship between the band structure and the catalytic property was examined. We expect such a metal−semiconductor nanocomposite may find some applications in the photocatalysis and antibacterial areas.

Experimental Section

In a typical procedure, zinc oxide nanofibers containing various contents of Ag can be prepared by first dissolving polyvinylpyrrolidone (PVP M_n 1 300 000, Alfa Co.) in absolute ethanol and then mixing well with a mixture of zinc nitrate ($Zn(NO_3)_2 \cdot 6H_2O$) and silver nitrate ($AgNO_3$) in deionized water by magnetic stirring. The weight ratio of the starting materials was $Zn(NO_3)_2 \cdot 6H_2O$/PVP/ethanol/H_2O = 4:3:30:10, and the Ag contents in the ZnO nanofibers were adjusted as 0, 1.0, 3.0, 5.0, 7.5, and 10.0 atom %, respectively. The setup for electrospinning was similar to that reported previously,[23] except for the configuration of the syringe, as illustrated in Figure S1a (see Supporting Information). Here, a plastic capillary with an inner diameter of 0.5 mm was used as the spinneret, and the electric field was applied by dipping a charged silver thread directly into the spinning solution. At an applied high voltage of 15 kV, a nonwoven mat of PVP/$Zn(NO_3)_2$/$AgNO_3$ composite fibers was collected on a grounded aluminum foil at an electrode distance of 15 cm. The as-spun nanofibers were then calcined at 520 °C in air for 1 h.

Rhodamine B (RhB) was employed as a representative dye indicator to evaluate the UV photocatalytic activity of Ag−ZnO nanofibers. For each condition, 10 mg of photocatalyst was ultrasonically dispersed in RhB aqueous solution (2.5×10^{-5} M, 10 mL, pH 5.4) and magnetically stirred in the dark for 30 min to ensure the adsorption/desorption equilibrium of RhB with the catalyst. The mixture was then loaded in an open beaker and continuously stirred during the exposure to UV light from a low-pressure Hg tube (Philips TUV 8 W; the strongest emission at 254 nm). The setup for the photocatalytic measurement was shown in Figure S1b (Supporting Information), and the whole photocatalytic reaction took place at room temperature. UV−vis absorption spectra of samples were measured at regular intervals of 10 min to monitor the reaction, and the absorption at 554 nm was recorded as a function of irradiation time.

The morphology and composition of the products were characterized by transmission electron microscopy (TEM, JEOL-2011, Tokyo, Japan) and scanning electron microscopy (SEM, JEOL JSM-6460LV, Tokyo, Japan) equipped with energy dispersive X-ray analysis (EDX). X-ray diffraction (XRD, D/MAX-RB X-ray diffractometer, Rigaku, Akishima-Shi, Japan) was used to analyze the crystalline structure of the ZnO nanofibers with various Ag contents. X-ray photoelectron spectroscopy (XPS, PHI-5300 ESCA, U.S.A.) was used mainly for the analysis of elemental and chemical states of silver in this heterostructure. Photoluminescence (PL, Renishaw 1000, U.K.) was measured at room temperature using a He−Cd laser as the excitation light source, at a wavelength of 325 nm.

In the investigation of the aqueous suspensions of Ag−ZnO nanofibers, the electrophoretic measurement was performed using a zeta potential analyzer (Zeta Plus V3.57, Brookhaven Instruments Corporation, U.S.A.) to determine the isoelectric points (IEP) of the photocatalysts. Suspensions containing 0.2 g L^{-1} of Ag−ZnO in deionized distilled water were treated in the ultrasonic bath for 1 h and then stored for 24 h. Such a low oxide concentration was used to avoid hydrodynamic and electrostatic interaction between particles.[24] pH values were adjusted by addition of ammonia and acetic acid respectively.

Results and Discussion

As the TG/DSC results reveal almost no weight loss and heating effect above 450 °C (see Supporting Information, Figure S2), the yielded nonwoven mat of precursor fibers was annealed in air at 520 °C for 1 h to obtain Ag−ZnO nanofibers on the basis of the following chemical reactions:

$$2Zn(NO_3)_2 \rightarrow 2ZnO + 4NO_2\uparrow + O_2\uparrow \quad (1)$$

$$2AgNO_3 \rightarrow 2Ag + 2NO_2\uparrow + O_2\uparrow \quad (2)$$

It is obvious that the as-spun nanofibers (Figure 1a) are smooth and uniform in terms of diameter, while the diameters of the calcined one (Figure 1b) have shrunk markedly to 80−150 nm. The EDX spectrum of Ag−ZnO nanofibers (inset of Figure 1b) prepared with a silver concentration of 5.0 atom % confirms the presence of both silver and zinc with an atomic ratio of ~1:20.

Transmission electron microscopy (TEM) was used to observe the distribution of the Ag particles, shown in Figure 2. As compared with the pure ZnO nanofibers (see Figure S3, Supporting Information), no distinct change was observed on the morphology of the 5.0 atom % Ag−ZnO sample except for the dispersion of various Ag

(17) Yu, Y. X.; Xu, D. S. *Appl. Catal., B* **2007**, *73*, 166–171.
(18) Liu, Z. Y.; Sun, D. D.; Guo, P.; Leckie, J. O. *Nano Lett.* **2007**, *7*(4), 1081–1085.
(19) Zhan, S. H.; Chen, D. R.; Jiao, X. L.; Song, Y. *Chem. Commun.* **2007**, *20*, 2043–2045.
(20) Patel, A. C.; Li, S. X.; Wang, C.; Zhang, W. J.; Wei, Y. *Chem. Mater.* **2007**, *19*, 1231–1238.
(21) Jin, M.; Zhang, X. T.; Nishimoto, S.; Liu, Z. Y.; Tryk, D. A.; Emeline, A. V.; Murakami, T.; Fujishima, A. *J. Phys. Chem. C* **2007**, *111*, 658–665.
(22) Chen, L.; Bromberg, L.; Hatton, T. A.; Rutledge, G. C. *Polymer* **2007**, *48*, 4675–4682.
(23) Lin, D. D.; Wu, H.; Pan, W. *Adv. Mater.* **2007**, *19*(22), 3968–3972.
(24) Gun'ko, V. M.; Zarko, V. I.; Leboda, R.; Chibowski, E. *Adv. Colloid Interface Sci.* **2001**, *91*, 1–112.

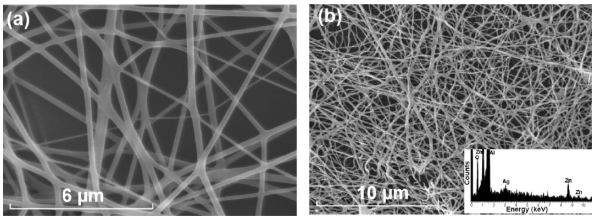

Figure 1. SEM images of (a) as-spun $AgNO_3/Zn(NO_3)_2$/PVP fibers and (b) the fibers annealed at 520 °C for 1 h in air (the inset shows the EDX spectrum of ~5.0 atom % Ag−ZnO nanofibers).

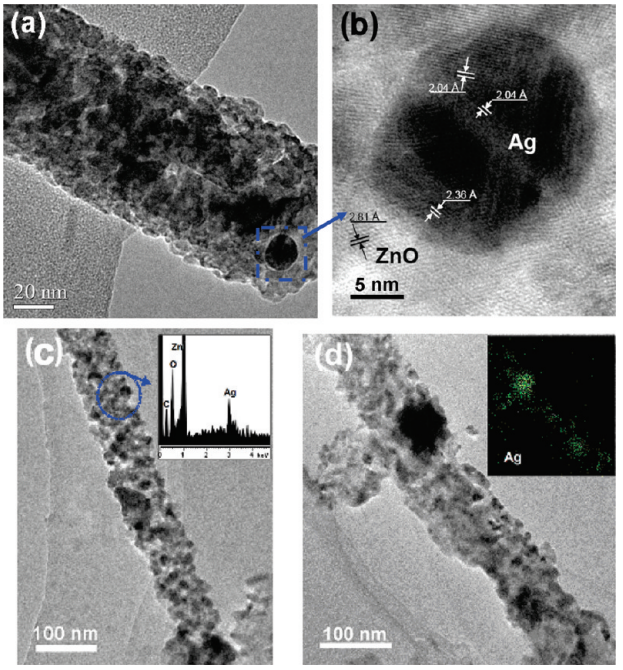

Figure 2. TEM images of Ag−ZnO nanofibers with various Ag content. (a) Ag-5.0 atom %; (b) HRTEM image from the squared region of part a; (c) Ag-7.5 atom % (insets: typical EDX microanalysis on selected areas of a single nanowire, showing that the single nanowire was indeed composed of Ag nanoparticles and ZnO matrix); and (d) Ag-10 atom % (inset: EDX mapping of Ag element along the nanowire).

nanoparticles in the size range from several to 12 nm throughout the volume of the nanofibers (Figure 2a). When a single particle is imaged at high resolution, as shown in Figure 2b, the crystal lattice can be observed directly, with spacing d of 2.36 Å and 2.04 Å. This corresponds to Ag(111) and (200), in good agreement with the card JCPDS No. 04-0783, strong evidence for the existence of metallic Ag nanoparticles. Figure 2c reveals a uniform and separate distribution of Ag particles (black dots) in the ZnO matrix (gray region) of the 7.5 atom % Ag−ZnO nanofibers. The EDX spectrum recorded from the selected area reveals the composition, including Ag and Zn. Further increase of silver content (10 atom %) induces local aggregation of Ag particles, which can be observed by the EDX mapping of elemental Ag through the nanofiber (Figure 2d).

Figure 3 shows XRD spectra of Ag−ZnO nonwovens with various Ag content. The peaks at 2θ values of 31.77°, 34.42°, 36.25°, 47.54°, 56.60°, and 62.86° (marked with #) observed in all samples are indicative of the typical hexagonal wurtzite structure of ZnO (according to

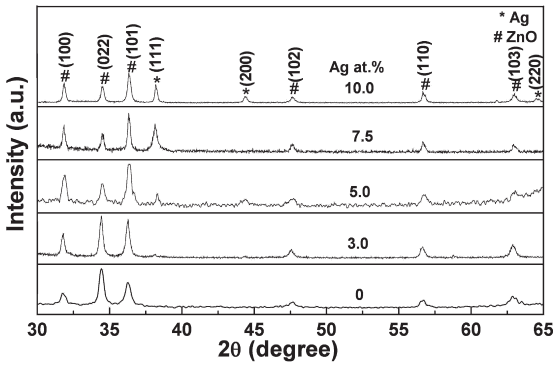

Figure 3. XRD patterns of the Ag−ZnO nanofibers with various Ag concentrations.

JCPDS No. 36-1451 for ZnO), while those of 38.20°, 44.40°, and 64.60° can be indexed to fcc metallic Ag (marked with *). No peaks corresponding to Ag_2O are detected. With the addition of Ag content, the diffraction peaks of ZnO shift slightly to the right, implying an increase of defects that may arise from the Ag−ZnO interface.[25] Besides, as calculated by the Scherrer equation ($L = 0.89\lambda/(\beta \cos \theta)$, L is the average particle size in Å, β the full width of the peak at half-maximum, and θ the diffraction angle), the average crystallite size of ZnO is in the range of 14−19 nm, while the grain of Ag grows remarkably as a result of the aggregation at high silver content.

To clarify the elemental and chemical state of Ag in the sample, XPS spectra were introduced. Figure 4a shows that the Ag−ZnO nanofibers collected on the foam nickel contain not only Zn, O, and Ag elements but also some Ni and C elements. The XPS peak for Ni is obviously ascribed to the collector material, while C 1s at E_b = 284.8 eV is due to the hydrocarbon from the XPS instrument itself.[26] Figure 4b provides the high-resolution XPS spectra of Ag in the Ag−ZnO composite. The Ag $3d_{5/2}$ peak appears at a binding energy of 367.4 eV, and the splitting of the 3d doublet is 6.1 eV, indicating the metallic nature of silver.[27] Here, interestingly, the $3d_{5/2}$ peak of Ag in our work was found to shift obviously to the lower binding energy compared with the standard value (about 368.2 eV for bulk Ag). This confirms the interaction between Ag and ZnO nanocrystals as the binding energy of monovalent Ag is known to be much lower than that of zerovalent Ag. Similar results were also found in Zheng's work.[15]

The photocatalytic activities of the pure ZnO and Ag−ZnO nanofibers with various silver contents were evaluated by the degradation of RhB dye under UV irradiation. Typical morphology of the photocatalyst dispersed in the solution is shown in the inset of Figure 5a. Those fibril structures facilitate the dispersion

(25) (a) Kuo, S. T.; Tuan, W. H.; Shieh, J.; Wang, S. F. *J. Eur. Ceram. Soc.* **2007**, *27*(16), 4521–4521. (b) Fan, J. W.; Freer, R. *J. Appl. Phys.* **1995**, *77*(9), 4795–4800.
(26) Yu, J. G.; Xiong, J. F.; Cheng, B.; Liu, S. W. *Appl. Catal., B* **2005**, *60*, 211–221.
(27) Moudler, J. F.; Stickle, W. F.; Sobol, P. E.; Bomben, K. D. *Handbook of X-ray Photoelectron Spectroscopy*; Perkin-Elmer: Eden Prairie, MN, 1992.

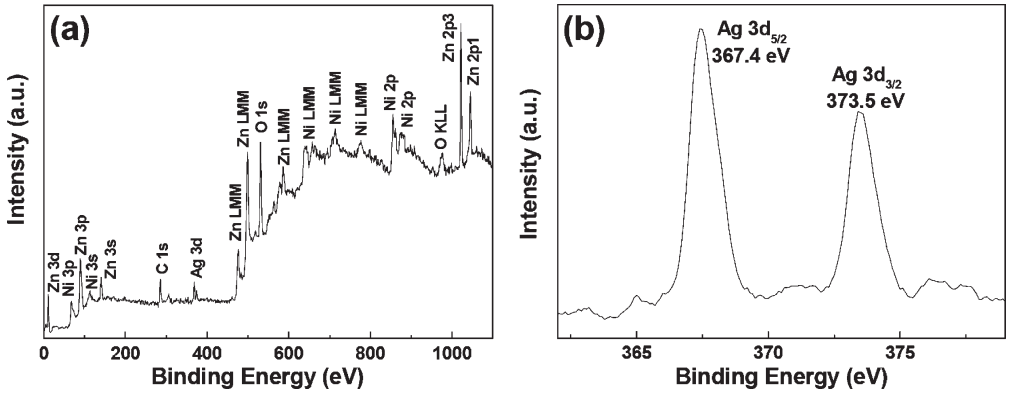

Figure 4. XPS spectra of the Ag−ZnO nanofibers obtained in the presence of 7.5 atom % Ag: (a) full spectrum of the sample and (b) Ag 3d spectrum.

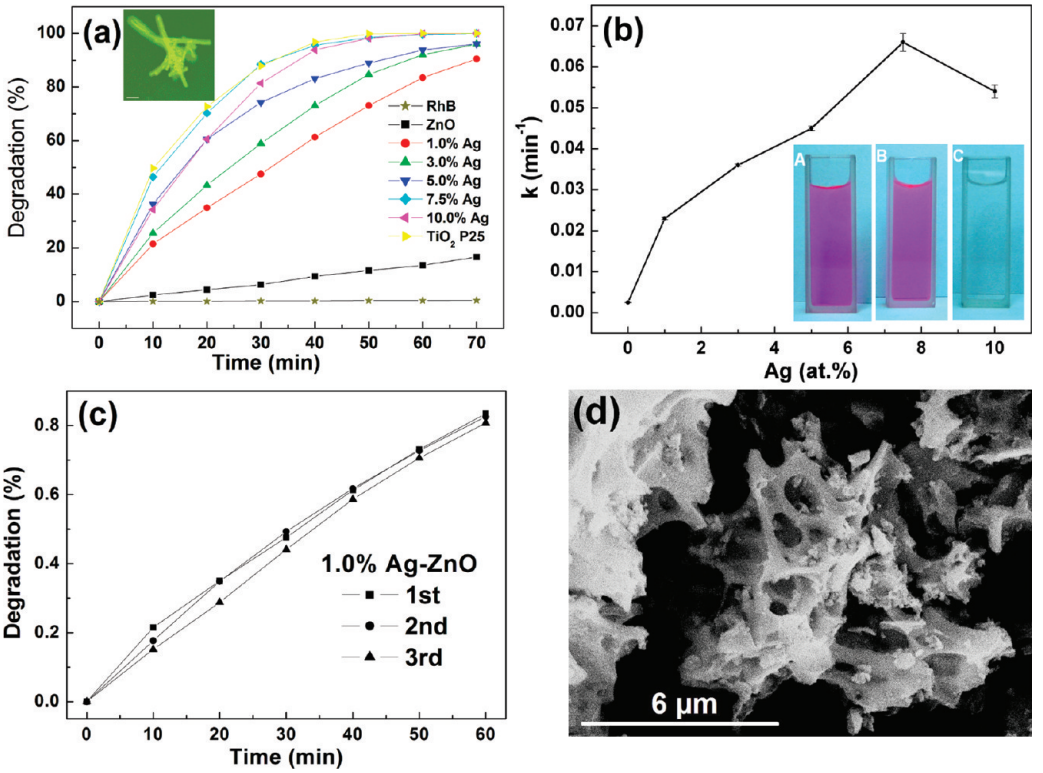

Figure 5. (a) Kinetics of the photodegradation of an aqueous solution of RhB by Ag−ZnO heterojunction nanofibers. The inset was the typical morphology of the photocatalyst dispersed in the dye solution (scale bar: 5 um). (b) Degradation rate constants for Ag−ZnO nanofibers obtained in the presence of different Ag contents (the inset illustrates photos for comparison of the RhB solutions photodegraded with various Ag−ZnO nanofibers for 70 min; A, without catalyst; B, pure ZnO; and C, 7.5 atom % Ag−ZnO). (c) The repeatability tests studied on the 1.0 atom % Ag−ZnO sample for three recycles. (d) The SEM image of the sample reclaimed after photocatalytic measurement.

and the maximum contact of nanofibers and the reagent, which makes Ag−ZnO the ideal candidate for catalytic application. In Figure 5a, the blank test shows that the concentration of RhB changes little after irradiation, indicating that the photoinduced self-decomposition can be neglected in comparison with the photocatalysis caused by catalyst particles. Moreover, the result shown in Figure S4 further indicates that the electron injection from photoexcited RhB molecules to Ag−ZnO is poor and neglectable, excluding the influence of the self-sensitized photolysis by dyes as well as the role of Ag−ZnO catalyst in electron-transfer mediation. Thus, the UV-light-induced degradation of RhB in our work can be evaluated as a real photocatalytic activity of the Ag−ZnO catalyst. When Ag was coupled in ZnO nanofibers, a remarkable enhancement in photocatalytic activity was observed. The optimal loading of Ag is around 7.5 atom % as the RhB is almost completely degraded when irradiated for 50 min, which is comparable to the commercial TiO_2 (Degussa P-25). The photodegradation of RhB can be considered as a pseudo-first-order reaction,[18,28] and its kinetics can be expressed as follows

$$C = C_0 e^{-kt} \quad (3)$$

(28) Wan, Q.; Wang, T. H.; Zhao, J. C. *Appl. Phys. Lett.* **2005**, *87*, 083105–083107.

where k is the degradation rate constant and C_0 and C are the initial concentrations of RhB and that at the reaction time t, respectively. The sample with 7.5 atom % Ag shows the highest catalytic activity with rate constant (k) of 0.024 min^{-1}, about 25 times more than that of pure ZnO nanofibers (0.0025 min^{-1}), as shown in Figure 5b. More intuitively, the color of RhB solution photodegraded with pure ZnO nanofibers for 70 min changes little (inset of Figure 5b: B) while the one with Ag−ZnO (7.5 atom %) turns to be colorless and clear (inset of Figure 5b: C), as compared with the original solution (inset of Figure 5b: A). The improved activity was generally attributed to the efficient charge separation of Ag−ZnO composite relative to pure ZnO. Moreover, the sample (1.0 atom % Ag) with 3-time recycles indicates no obvious decrease for photocatalytic activity (Figure 5c). The catalyst recovered from reaction still preserves the three-dimensional open structure, although some of them are broken up into smaller pieces during the ultrasonic suspension and centrifugal separation process (Figure 5d). This fact that the fibril photocatalysts with high photocatalytic activity can be easily recovered will greatly promote their industrial application to eliminate the organic pollutants from wastewater.

As the photocatalytic process of the Ag−ZnO composite is complex and controversial, here we would like to discuss it in detail by proposing the band structure of the Ag−ZnO heterojunction. It is known that the work function of ZnO (5.2 eV) is larger than that of Ag (4.26 eV), implying that the electrons will migrate from silver to the conduction band (CB) of ZnO to achieve the Fermi level equilibration when they get into contact. The process can be expressed as

$$Ag \rightarrow Ag^{+} + e^{-} \quad (4)$$

When the catalysts are illuminated by UV light with photon energy higher than the band gap of ZnO, electrons (e^-) in the valence band (VB) can be excited to the CB with simultaneous generation of the same amount of holes (h^+) left behind. The scheme for the photocatalytic process is shown in Figure 6. In the Ag−ZnO system, the deflexed energy band in the space charge region facilitates the rapid transfer of the as-excited electrons from ZnO to Ag nanoparticles, which increases the lifetime of the photogenerated pairs. Electrons accumulated at Ag particles or the conduction band of ZnO can be transferred to oxygen molecules adsorbed on the surface to form free oxygen radicals, such as $^{\bullet}O^{-}_2$, $^{\bullet}HO_2$, $^{\bullet}OH$, and so forth,[26] while the photoinduced holes are apt to react with surface-bound H_2O or OH^- to produce the hydroxyl radical species ($^{\bullet}OH$) which is an extremely strong oxidant for the mineralization of organic chemicals. Besides, the defects at the Ag−ZnO interface have also been demonstrated to suppress the charge recombination by transferring the photogenerated electrons to the dye in solution.[15]

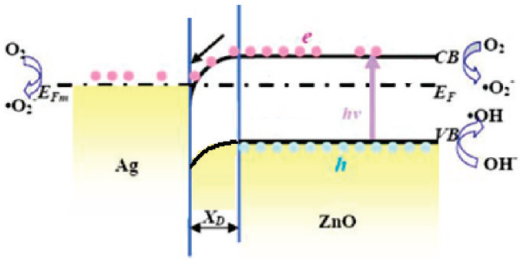

Figure 6. Proposed schematic illustrations of the band structure related photocatalytic mechanism for the Ag−ZnO heterojunction.

The photocatalytic reaction can be thus expressed as follows:[29]

$$ZnO + h\nu \rightarrow e^{-} + h^{+} \quad (5)$$

$$h^{+} + OH^{-} \rightarrow {}^{\bullet}OH \quad (6)$$

$$h^{+} + H_2O \rightarrow {}^{\bullet}OH + H^{+} \quad (7)$$

$$e^{-} + Ag^{+} \rightarrow Ag \quad (8)$$

$$e^{-} + O_2 \rightarrow {}^{\bullet}O^{-}_2 \quad (9)$$

$${}^{\bullet}O^{-}_2 + H^{+} \rightarrow {}^{\bullet}OH2 \quad (10)$$

$$2{}^{\bullet}OH2 \rightarrow H_2O_2 + O_2 \quad (11)$$

This proposed mechanism can be supported by the photoluminescence (PL) spectra. As shown in Figure 7, the room-temperature PL spectra of Ag−ZnO comprise two emission bands in the UV/visible regions under the above band-edge excitation. The narrow UV emission band centered at 369 nm is assigned to the exciton recombination while the violet one centered at 410−420 nm originates from some interface traps of radiative defects at the grain boundaries between silver and ZnO grains.[30] With the addition of silver, the PL intensity in the ultraviolet region is almost quenched as a result of the charge transfer from ZnO to Ag, which provides additional evidence that the noble-metal contact improves the energetics of the semiconductor-assisted photocatalysis. In addition, the violet emission intensity decreases when the Ag content exceeds 5.0 atom %. The change can be mainly attributed to the absorption or reflection of emission at the Ag/ZnO interface, which is induced by the strong surface plasmon absorption of Ag nanoparticles at ~410 nm.[31,32]

Measurement of the zeta (ξ)-potential of Ag−ZnO nanofibers was also carried out to further confirm some details regarding the adsorption of RhB dye and

(29) Lu, H. B.; Li, H.; Liao, L.; Tian, Y.; Shuai, M.; Li, J. C.; Hu, M. F.; Fu, Q.; Zhu, B. P. *Nanotechnology* **2008**, *19*, 045605–045611.
(30) Zhao, S. Q.; Zhou, Y. L.; Zhao, K.; Liu, Z.; Han, P.; Wang, S. F.; Xiang, W. F.; Chen, Z. H.; Lu, H. B.; Cheng, B. L.; Yang, G. Z. *Physica B* **2006**, *373*, 154–156.
(31) Yang, L.; Li, G. H.; Zhang, L. D. *Appl. Phys. Lett.* **2000**, *76*(12), 1573–1575.
(32) He, R.; Qian, X. F.; Yin, J.; Zhu, Z. K. *J. Mater. Chem.* **2002**, *12*, 3783–3786.

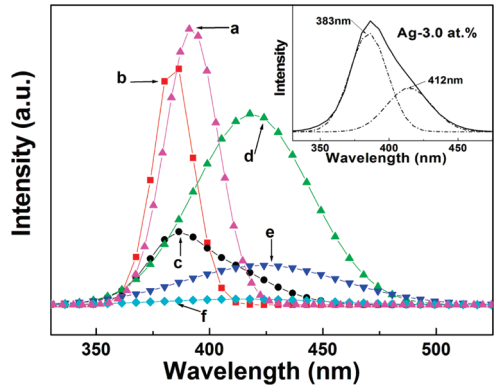

Figure 7. PL spectra of the Ag−ZnO nanofibers with various Ag contents: (a) pure ZnO, (b) 1.0 atom % Ag, (c) 3.0 atom % Ag, (d) 5.0 atom % Ag, (e) 7.5 atom % Ag, and (f) 10.0 atom % Ag. The inset shows the Gaussian fitting of curve c.

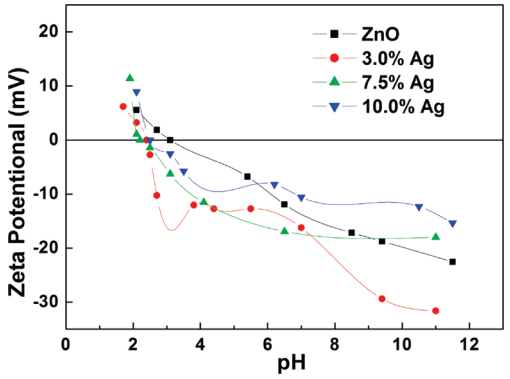

Figure 8. Zeta potential of Ag−ZnO nanowires with various silver concentrations as a function of pH value.

hydroxide ions on the catalyst surface. In Figure 8, it can be found that the lowest isoelectric point (where the zeta-potential is 0) occurs at pH 2.0 for the 7.5 atom % Ag−ZnO, which means more efficient adsorption of the cationic RhB as well as a higher concentration of hydroxide ions on the surface of the catalyst. Hydroxide ions act as hole traps that prevent electron−hole recombination, creating a higher quantum yield, and thus result in a higher photocatalytic reaction rate.[33,34]

When the Ag content exceeds 7.5 atom %, the number of active sites capturing the photoinduced electron is decreased with an aggregation of Ag particles. Moreover, excessive Ag can shield the UV light adsorption by ZnO, deteriorating the photon utilizing efficiency.[35] As an overall effect, the photocatalytic activity of the catalyst is therefore depressed, which is in good agreement with the observations discussed above. The features presented here highlight the importance of designing semiconductor−metal composite nanostructures for light energy harvesting applications.

Conclusion

In conclusion, photocatalytically active Ag−ZnO composite nanofibers have been successfully prepared via a simple electrospinning process, followed by thermal treatment to remove the PVP and to convert silver nitrate to silver nanoparticles. The resultant heterostructure could promote the charge separation of the photogenerated electrons (e^-) and holes (h^+), allowing both of the e^- and h^+ participating in the overall photocatalytic reaction. The optimal photocatalytic activity of Ag−ZnO nanofibers exceeded that of pure ZnO nanofibers by a factor of more than 25 when the Ag concentration was kept at 7.5 atom %. Therefore, exploring the catalytic activity of such composite structures may pave the way for designing useful nanoscale building blocks for photocatalytic and photovoltaic applications.

Acknowledgment. This study was supported by the National Natural Science Foundation of China (Grant 50872063).

Supporting Information Available: Experimental and characterization details (PDF). This material is available free of charge via the Internet at http://pubs.acs.org.

(33) Hu, C.; Wang, Y. Z.; Tang, H. X. *Appl. Catal., B* **2001**, *30*, 277–285.
(34) Yu, J. C.; Lin, J.; Kwok, R. W. M. *J. Photochem. Photobiol., A* **1997**, *111*, 109–203.
(35) (a) Wang, H. Y.; Niu, J. F.; Long, X. X.; He, Y. *Ultrason. Sonochem.* **2008**, *15*, 386–392. (b) Méndez, M. A.; Cano, A.; Suárez, M. F. *Ultrason. Sonochem.* **2007**, *14*, 337–342.